14th Australasian Fluid Mechanics Conference
Adelaide University, Adelaide, Australia
10-14 December 2001

Comparisons of Isothermal and Combusting Jets

C. P. Syred and T. O'Doherty

Division of Mechanical Engineering and Energy Studies

Cardiff University, Wales, CF24 0YF, UK

Abstract

This study looks at the fundamentals of turbulent free jets under isothermal and combustion conditions. The turbulent characteristics and structure of the flow are examined, and the effects of scale between different jet sizes investigated.
Comparisons of isothermal and combusting turbulent, free jets at different scales and Reynolds numbers were made, using results taken with LDA and PIV measuring techniques. Each nozzle had a constant exit velocity of 16m/s, with Reynolds numbers between 10000 and 20000. The nozzles have diameters of 10, 15 and 20mm. Acetylene was used as the fuel for the combustion jets, and was introduced upstream of the nozzle exit. Measurements were concentrated in the near field region of flow close to the jet exit, to a distance of X/D=5 downstream of the nozzle exit.
The basic aerodynamic characteristics for each jet was identified from the mean velocity and turbulence profiles determined from LDA measurements. The small-scale turbulent structures and length scales were determined for each jet from PIV data, time correlations and energy spectrums.
The structure and turbulent properties for each jet size are compared, and using velocity-scaling techniques scaling criteria investigated.

Introduction

Scaling is a problem in all engineering combustion systems. Over the years different scaling techniques have been used to model large systems from smaller ones. Tests on small-scale laboratory size burners have been used to predict the performance of larger units. However experience has shown that scaling combustion systems can be unreliable, [5,6,7,10]. Therefore reliable methods are needed in order to predict the performance of large-scale systems from smaller ones.
Several different modelling systems are used to study burner scaling, and involve analytical models, Computational Fluid Dynamics (CFD) and scaling criteria. Although CFD is a useful tool for combusting flows, an initial model is still required for scaling purposes. This paper aims to investigate the effects of scale by comparing isothermal and combusting jets via their velocity and turbulent characteristics.
When considering burner design, scaling criteria's is generally used to model the burner. The two most commonly used scaling techniques in industrial burner design are constant velocity and constant residence time-scaling criteria. When dealing with different fuels, liquid, gas or solid, different scaling criteria are used under varying conditions. This paper investigates constant velocity scaling.

Constant Velocity Scaling

Constant velocity scaling requires that velocity is kept constant at the nozzle exit for different scale. Changes in scale results in changes in Reynolds number. Subtle changes occur in the turbulent structure and differences occur in the turbulent scales and mixing. Change in scale also cause different relative boundary layer effects, for example, the boundary layer becomes relatively thinner at large scale. These changes in parameters with different size, allows the effects of scale to be investigated.
The burner and flame scale are defined from the burner throughput: $Q_0 \propto \rho_0 U_0 D_0^2$
When a burner is scaled down from a baseline throughput, $Q_{0,base}$ to a reduced scale $Q_{0,scaled}$ the following scaling criteria can be derived, assuming the same system density:

$$\frac{Q_{0,base}}{Q_{0,scaled}} = \left(\frac{D_{0,base}}{D_{0,scaled}} \right)^2 \tag{1}$$

For constant velocity scaling where U_0=constant

Turbulent scales

Turbulent motion occurs due to velocity gradients in viscous flow, the mixing of streams of different velocities in the shear flow causes the formation of eddies. Turbulent flow consists of eddies of various sizes. The greater the range of eddy sizes the more turbulent the flow is. The largest eddies result from instabilities in the main flow, and derive their energy directly from it. These eddies have the dimension of the entire flow. The largest eddies break down, due to viscosity effects in the flow, and result in the conversion of its kinetic energy into heat. The fluid's energy dissipates, increasing the internal energy of the fluid. The larger eddies transfer energy to the smaller eddies. The process ends when all the energy in the smallest eddy is dissipated. The large eddies break down into small eddies by participating in a cascade process, where the transmission in energy occurs from the largest eddies to the smallest ones. This is known as the 'inertial range', [2,9] and is a result of the action of inertial forces. The smallest eddies dissipate all their energy into internal energy.

Integral Length Scale I_L

The integral length scale defines the size of the mean value of the largest eddies and are those with low frequencies and large energy. The integral scale is in the energy containing eddy range, and has the same order of magnitude as the flow width. The large scales contain the most energy and dominate the transport of momentum, mass and heat [2].
Considering the correlation, R_t, between the fluctuating velocities in a given direction, at a fixed position in space at two different time intervals, the time correlation is defined by:

$$R_t = \frac{\overline{u_1'(t)u_2'(t+\tau)}}{\overline{u_1'(t)u_1'(t)}} \tag{2}$$

where u' is the fluctuating velocity.
The time correlation enables the determination of the Integral time scale, I_t, which defines the mean value of the largest eddies.

$$I_t = \int dt R(t) \tag{3}$$

The integral time scale is related to the Integral length scale as:

$$I_L = UI_t \tag{4}$$

where U is mean velocity

This is from the relationship of x=Ut, assuming Taylor hypothesis and the turbulence intensity is less than 25% [2].

Taylor Micro-Scale

The Taylor micro-scale, λ_T, is the average size of the smallest eddies, and can be determined by:

$$\lambda_T^2 = \frac{\overline{u'^2}}{\left(\frac{\partial u'}{\partial x}\right)^2} \tag{5}$$

Power Spectral Density

The power spectral density shows the level of energy in the flow and is related to the RMS velocity by:

$$2\int_0^\infty E(f)df = RMS^2 \tag{6}$$

Experimental Facilities

A free round jet, with 3 changeable nozzles, with a diameter of 10, 15 and 20mm was used. Acetylene was introduced upstream of the nozzle exit. The same value of mixture ratio was kept for each combusting jet. The air was also introduced upstream of the nozzle diameter through a rotameter to control the flow rate. The flow was seeded with Titanium Dioxide particles (TiO_2), mean diameter 1μc, enabling the LDA and PIV systems to determine the velocity and turbulence parameters of the flow. These particles are chosen to follow the path of the flow, and scatter light from the laser. The LDA system uses the frequency shift occurring between the laser and photo-detector collecting the samples to determine the velocity properties of the flow. The PIV system measures particle displacement between two successive pictures, to determine the instantaneous velocities of the flow. The TiO_2 was introduced using a fluidised bed with compressed air. The jet exit velocity, of 16m/s, was constant for each test. The jet exited the nozzle into non-constrained ambient surroundings.

LDA and PIV Configuration

Laser Doppler Anemometry (LDA) measurements were taken using a Dantec 3D system operating in 2D mode with a coherent Innova 70 series Argon-ion laser. Syred and O'Doherty [8] describes the LDA system, errors and seeding considerations in detail. The PIV system consists of a dual cavity Spectron SL456G Nd:YAG pulsed laser sheet which provides 350mJ laser pulses of 8ns duration with a repetition rate of 66.65ms (15Hz). Also a Dantec 80C42 PIV 700 CCD double image camera and a Dantec PIV Processor 2000 were used. McCluskey [3,4] describes this PIV system in further detail.

Results

Velocity and turbulence measurements were taken using LDA at various positions downstream of the nozzle exit, across the axis of the jet. Constant velocity of 16m/s was maintained at each nozzle exit. Figure 1 shows the mean axial and RMS fluctuating velocities for the 10mm isothermal nozzle at positions 1, 2 and 5 nozzle diameters downstream of the exit, normalised with respect to the exit axial velocity, U_0. At X/D=1 the mean axial velocity profile produces a typical "top hat" shape. The velocity and concentration across the centre of the jet has remained constant to that at the nozzle exit, the jet is in the potential core. At the edge of the jet there are steep velocity gradients. This is where the turbulent boundary layer has developed, also known as the "shear layer". The jet has entrained air from the surroundings by momentum and mass transfer into the shear layer. As the jet develops downstream more air is entrained and the shear layer grows across the jet. This can be seen at X/D=2, where the velocity gradient has become less steep, and the width of the jet has started to increase. At X/D=5, the centreline axial velocity has dropped below that of the exit velocity, hence the potential core has dissipated. This corresponds with results discussed in Beer and Chigier [1], which indicate the potential core of an isothermal jet lies between 4 and 5 nozzle diameters. The RMS fluctuating velocity profiles at X/D=1, show low levels across the centre of the jet, with peak values occurring in the shear layer (Figure 1).

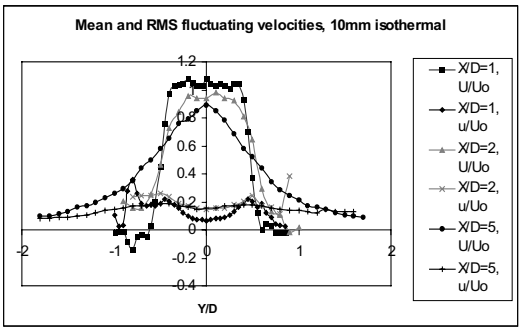

Figure 1. Mean axial and RMS fluctuating velocity profiles for 10mm nozzle at X/D=1,2 and 5 under isothermal conditions

This shows higher levels of turbulence in the edge of the jet, caused by the momentum and mass transfer. Eddies are formed in the flow due to viscosity effects and the kinetic energy in the flow is dissipated causing a cascade of energy, and the large eddies are broken down to smaller eddies causing a range of eddy sizes. As the jet develops downstream the RMS fluctuations increase across the jet as the shear layer expands, increasing the turbulence across the centre of the jet.

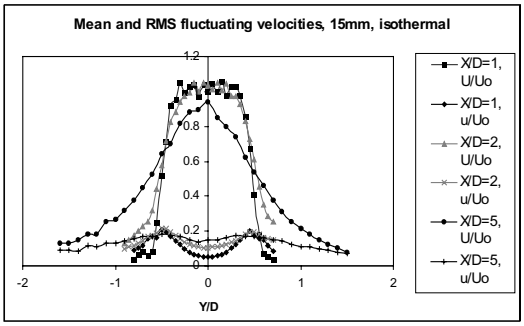

Figure 2. Mean axial and RMS fluctuating velocity profiles for 15mm nozzle at X/D=1, 2 and 5 under isothermal conditions

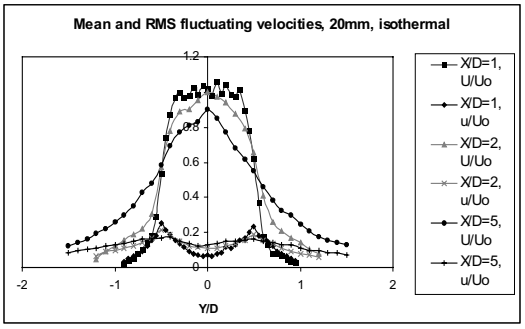

Figure 3. Mean axial and RMS fluctuating velocity profiles for 20mm nozzle at X/D=1, 2 and 5 under isothermal conditions

Figure 2 and 3 show the mean axial and RMS fluctuating velocity profiles for a 15 and 20mm nozzle diameter, respectively. The velocity profiles for the nozzles show very similar profiles to that of the 10mm nozzle, with the typical "top hat" profile identified at X/D=1, as the jets develop their shear layers grow and

turbulence increases across the jet. At X/D=5, the mean velocity profiles for the three nozzles show that on the centreline of the jet the velocities decay at the same rate, therefore the end of the potential core is at the same position for each nozzle.
From comparison of the three nozzles it can be concluded that under isothermal conditions the round free jet can be scaled with little change in their velocity characteristics.

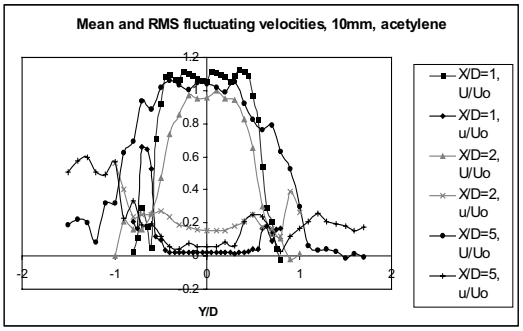

Figure 4. Mean axial and RMS fluctuating velocity profiles for 10mm nozzle at X/D=1, 2 and 5 under isothermal conditions

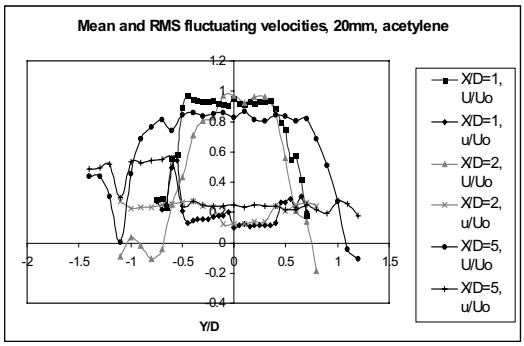

Figure 5. Mean axial and RMS fluctuating velocity profiles for 15mm nozzle at X/D=1, 2 and 5 under combustion conditions

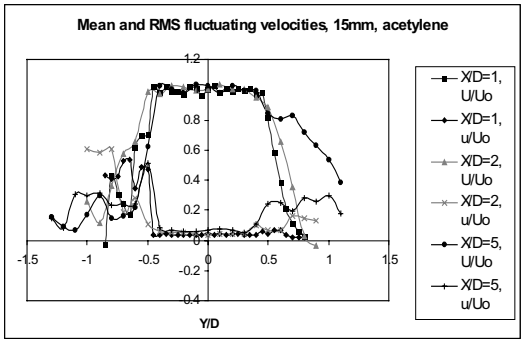

Figure 6. Mean axial and RMS fluctuating velocity profiles for 20mm nozzle at X/D=1, 2 and 5 under combustion conditions

Figures 4-6 show mean axial and RMS fluctuating velocity profiles for a combusting free jet, using acetylene as the fuel, for 10, 15 and 20mm nozzle exit diameters respectively. For each nozzle at X/D=1 the "top hat" velocity profile can be seen, and each jet is the same width, with steep velocity gradients occurring in the shear layer that has developed in the edge of the jet. However the RMS fluctuating velocities across the centre of the jet are not the same, and appear to increase, with increasing nozzle diameter. This indicates that the larger the nozzle diameter the more turbulent the jet, which corresponds to the higher Reynolds number. This however is not the case for the isothermal jet where the RMS fluctuating profiles are very similar showing the turbulent structure scales more closely than for the acetylene jets. Further downstream of the nozzle exit more air is entrained into the jet and the width of the jet spreads. The mean velocity across the centre of the jet does not decay at the same rate as the isothermal jet. This is primarily due to two processes, a) the acceleration effect due to combustion and changing gas viscosity and b) the higher jet edge velocities, which changes the entrainment and turbulence effects.
From the comparison of the three acetylene jets, it can be seen that at different scales, near the nozzle exit, the velocity characteristics have similar behaviour, however further downstream the velocities started to deviate from each other. The RMS fluctuating velocities differ in values across the jet at different scales showing differences in the turbulent structures.

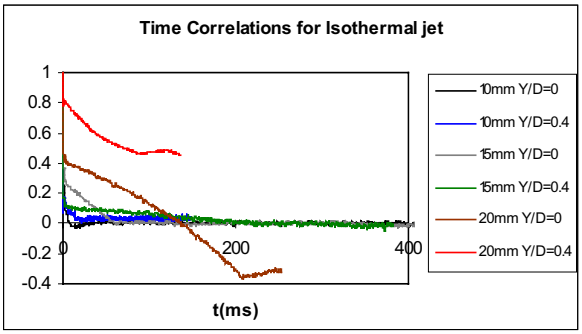

Figure 7. Time correlations for 10, 15 and 20mm nozzles at Y/D=0 and 0.4, under isothermal conditions

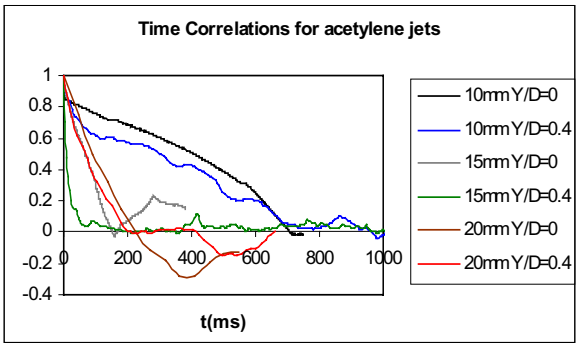

Figure 8. Time correlations for 10, 15, 20mm nozzles at Y/D=0 and 0.4, under combustion conditions

Figures 7 and 8 show the time correlation's at X/D=1 for the 10, 15 and 20mm nozzles for the isothermal and acetylene jets, respectively. The time correlation's enable the determination of the integral length scale, which is the average size of the largest eddies in the flow and should have a characteristic length of the order of the nozzle exit diameter. The largest eddies contain the most energy and dominate the transport of momentum, mass and heat. Using equation 4 the integral length scale, L_I, was calculated from the time correlation, equation 2. At Y/D=0, the integral length scale under isothermal conditions, for the 10mm nozzle, is 14mm. The time correlation's for the isothermal jets, generally shows increasing eddy size with scale. The 20mm nozzles along the centreline shows very large values of L_I, which shows that in the potential core, where there is little mixing, length scales are indicative of the upstream pipe conditions. However under combustion conditions the smaller scale, the jet with the 10mm nozzle, appears to have a bigger eddy size, than that of the larger nozzle. Also the eddy sizes are much larger for acetylene than for isothermal conditions. This shows that the acetylene jet has a different turbulent structure than the isothermal jet, and does not scale in the same way.
The gradient of the time correlation curve also gives information about the average eddy size. This average eddy size is known as the Taylor micro-scale and can be calculated from the initial gradient of the parabola of the curve, [2]. The steeper the gradient is the smaller the average eddy size. This calculation is only accurate if enough data is obtained around this point. As this was not the case the Taylor micro-scales were calculated by equation 5 from statistical results taken using PIV, at isothermal condition.

PIV could not be used to measure acetylene as the flame produced too much radiation, and hence was too luminous to be illuminated by laser light.

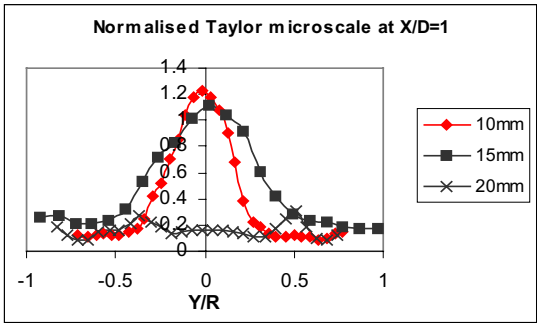

Figure 9. Taylor micro-scale for 10, 15 and 20mm nozzles across jet width, under isothermal conditions

Figure 9 shows the Taylor micro-scale at X/D=1, normalised with respect to the nozzle diameter, for the three nozzle sizes. The 10 and 15mm nozzles showed similar average eddy sizes, with the eddies in the centre being of the order of magnitude of the nozzle diameter. For the 20mm nozzle, there is a different turbulent micro-scale structure, which show the expected values of the Taylor micro-scales. Therefore PIV results for the 10 and 15mm nozzle are in error, this is due to insufficient data when considering mean values. This shows PIV is a useful tool for visualisation but not averaging unless very much larger data sets can be obtained.

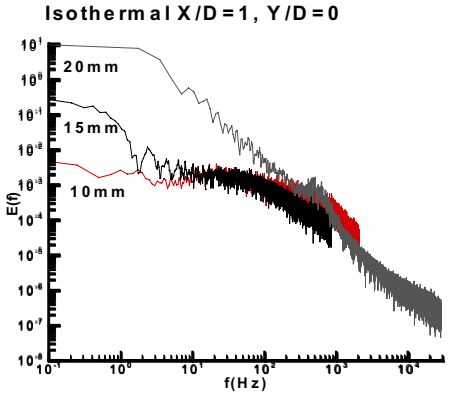

Figure 10. Power Spectral Density for 10, 15, 20mm nozzles at X/D=1 and Y/D=0 under isothermal conditions

Figure 10 and 11 show power spectra under isothermal conditions at X/D=1, for the 10, 15 and 20mm nozzle, at Y/D=0. The power spectrum shows levels of energy available at points in the flow. At low frequency, <10 Hz, data is invalid as very large sampling rates would be required to attain the expected spectrum [2]. However the energy spectrum is consistent with measured RMS values, equation 6. Therefore even more data than that collected at a greater data rate is needed to identify low frequency effects which the data appears to show. At Y/D=0 there is high levels of energy at low frequency, which correspond to the large eddies. The energy levels are larger for increasing scale, which correspond to the results shown in the time correlations, which show the integral length scale (the largest eddies) also increase with scale. The 10 and 15mm nozzles show similar levels of energy over higher frequency, which show a range of eddy sizes similar to each other. However the 20mm nozzle has a much larger range of eddy sizes, which is due to the jet having a different small scale turbulent structure than the other nozzles. This can be seen from the Taylor micro-scales, figure 9. The power spectrum for acetylene at Y/D=0 shows, that for each nozzle there is large energy at low frequency and there is a range of energy at higher frequencies for each nozzle size, showing a range of eddy sizes. Differences in levels at X/D=1 occur for isothermal and acetylene jets as reacting jets have much longer potential cores so are more stable over a greater range. The isothermal jet is greater influenced by breakup from the jet edge, which influences the middle, which is shown from the larger RMS values spreading across the jets centre.

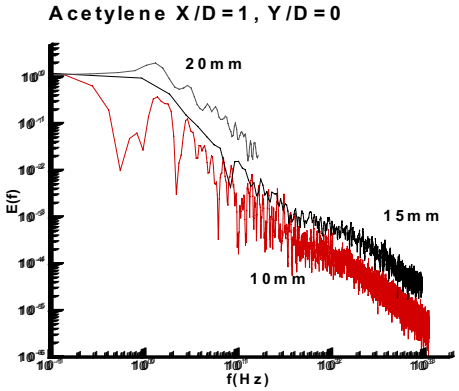

Figure 11. Power Spectral Density for 10, 15 and 20mm nozzles at X/D=1 and Y/D=0, under combustion conditions

Conclusions

From the results it can clearly be seen that using constant velocity criteria for the scaling of isothermal jets gives similar velocity characteristics and large scale turbulent structures, however the micro-scale structures vary as the scale differs, showing a difference in small scale turbulent structures. The acetylene jet shows that near the nozzle exit the velocity structures scale, however the turbulence levels are larger with increasing scale. As the jet moves further from the exit, deviation between the velocities and turbulence structures occur. The micro-scale structure of the jets do not scale, showing a different turbulent structure. It can be seen from these conclusions, that when considering scaling parameters for burner design many different variables need to be taken into consideration. Investigation between large and small scale turbulence structures when scaling jets needs to be made, to be able to determine more precise scaling criteria.

References

[1]Beer, J. M. & Chigier, N. A., Combustion Aerodynamics, Applied Science Publishers, London, 1972

[2]Hinze, J. O., Turbulence. An Introduction to its Mechanism and Theory, McGraw-Hill, 1975

[3]McCluskey, D. R., Obtaining high-resolution PIV vector maps in real-time, International workshop om PIV, Fukui, Japan, 1995

[4]McCluskey, D. R. & Jacobsen, T., Instrumentation for real-time PIV measurements, Joint ASME, JSME & EALA conf. USA 1995

[5]Salvi, G., Combustion system scaling. IFRF, Report D07/a/69, 1979

[6]Smart, J.P., Some simple considerations on the turbulent mixing process in relation to flame scaling. Journal of the Institute of Energy, Sept 1998, 71, pp 152-155

[7]Smart, J.P., On the effect of burner scale and coal quality on low NO_x burner performance. PhD Thesis, Uni. of London, 1992

[8]Syred, C and O'Doherty, Physical Scaling and Modelling of a Free Jet Burner, 6th int. conf. on *Technologies and Combustion for a Clean Environment,* 2001

[9]Tennekes, H. & Lumley, J. L., A first course in Turbulence, The MIT Press, 1972

[10]Weber, R. (1996). Scaling characteristics of aerodynamics, heat transfer, and pollutant emissions in industrial flames. 26th symp (int) on Combustion, The Combustion Institute, pp 3343-3354